Ultrastructure of the Calcium Release Channel of Sarcoplasmic Reticulum

Akitsugu Saito,* Makoto Inui,* Michael Radermacher, Joachim Frank, and Sidney Fleischer*

*Department of Molecular Biology, Vanderbilt University, Nashville, Tennessee 37235; and Wadsworth Center for Laboratories and Research, New York State Department of Health, Albany, New York 12201

Abstract. This study is concerned with the characterization of the morphology of the calcium release channel of sarcoplasmic reticulum (SR) from fast-twitch skeletal muscle, which is involved in excitation–contraction coupling. We have previously purified the ryanodine receptor and found it to be equivalent to the feet structures, which are involved, in situ, in the junctional association of transverse tubules with terminal cisternae of SR. The receptor is an oligomer of a single high molecular weight polypeptide and when incorporated into phospholipid bilayers, has channel conductance which is characteristic of calcium release in terminal cisternae of SR. The purified channel can be observed by electron microscopy using different methods of sample preparation, with complementary views being observed by negative staining, double staining, thin section and rotary shadowing electron microscopy. Three views can be observed and interpreted: (*a*) a square face which, in situ, is junctionally associated with the transverse tubule or junctional face membrane; (*b*) a rectangle equivalent to the side view; and (*c*) a diamond shape equivalent to the side view, of which the base portion appears to be equivalent to the transmembrane segment. Negative staining reveals detailed substructure of the channel. A computer averaged view of the receptor displays fourfold symmetry and ultrastructural detail. The dense central mass is divided into four domains with a 2-nm hole in the center, and is enclosed within an outer frame which has a pinwheel appearance. Double staining shows substructure of the square face in the form of parallel linear arrays (six/face). The features of the isolated receptor can be correlated with the structure observed in terminal cisternae vesicles. Sections tangential to the junctional face membrane reveal that the feet structures (23-nm squares) overlap so as to enclose smaller square spaces of ~14 nm/side. We suggest that this is equivalent to the transverse tubule face and that the terminal cisternae face is smaller (~17 nm/face) and has larger alternating spaces as a consequence of the tapered sides of the foot structures. Image reconstruction analysis appears to be feasible and should provide the three-dimensional structure of the channel.

THE signal for calcium release in excitation–contraction coupling is transferred from transverse tubule across the triad junction to terminal cisternae of sarcoplasmic reticulum (SR)[1] (7, 22). Recently, significant progress has been made with regard to defining the molecular detail of the calcium release process (1, 8, 14–19, 27). The approach of our laboratory has been to isolate and characterize defined subcellular fractions from muscle (6). Subcellular fractions have been isolated referable to triads (20) as well as terminal cisternae of SR (25). Terminal cisternae differ from heavy SR in that they contain two types of membranes, i.e., the calcium pump membrane (~85% of the membrane) and the junctional face membrane containing well defined feet structures. The isolated terminal cisternae are leaky to calcium ions, whereas light SR, which are referable to longitudinal tubules of SR and consist only of calcium pump membrane, are impermeant to Ca^{2+} (2, 3). Ruthenium red (micromolar concentration) has been found to decrease the permeability to calcium ions in the terminal cisternae of SR (3) (see also 21) and ryanodine in nM concentrations was found to block this action of ruthenium red (8). The binding of ryanodine has been localized to terminal cisternae of SR. The pharmacological action of ryanodine and the binding occur in the same concentration range and are localized to the terminal cisternae of SR (8, 17). These studies lead to the conclusion that ryanodine modulates the calcium release channel of SR and that calcium release is localized to the junctional face membrane of the terminal cisternae of SR.

The ryanodine receptor has been purified and found to consist mainly of a single high molecular mass polypeptide with Stokes radius of 360 kD (15–17). The purified ryanodine receptor approximates a square structure (~25 nm/side) with a width of 12 nm, which is morphologically equivalent to the feet structures observed in the junctional face membrane (17, 18). Moreover, the purified receptor incorporated into phospholipid bilayers displayed the conductivity characteristics of the calcium release process of SR (14). Hence, the calcium release channel of SR has been identified to be

1. *Abbreviation used in this paper*: SR, sarcoplasmic reticulum.

the feet structures which are involved in junctional association to form the triad junction.

This study is concerned with the characterization of the ultrastructure of the calcium release channel and the nature of its association with the junctional face membrane.

Materials and Methods

Purification of Ryanodine Receptor (Calcium Release Channel of SR)

The ryanodine receptor from rabbit fast twitch skeletal muscle was purified from junctional terminal cisternae SR vesicles (25) as described previously (17) with some modifications (16). Briefly, junctional terminal cisternae vesicles were solubilized with CHAPS and soybean phospholipid in 0.3 M sucrose, 1 M NaCl, 2 mM dithiothreitol (DTT), 0.5 μg/ml leupeptin, and Tris-HCl, pH 7.4. The CHAPS extract was diluted to reduce the NaCl concentration to 0.1 M, and loaded onto an Affi-Gel heparin (BioRad Laboratories, Richmond, CA) column. The elution was achieved with a linear salt gradient (0.1–0.8 M NaCl). The ryanodine receptor enriched fractions were collected, and applied to a hydroxylapatite column. The receptor was eluted with a K-phosphate linear gradient (5–250 mM K-phosphate). The pooled fractions from the hydroxylapatite column were concentrated to ~1 ml using a Centriprep 30 (Amicon, Danvers, MA) and applied to a Superose 6 column (Pharmacia Biotechnology, Inc., Piscataway, NJ) pre-equilibrated and eluted in 0.5 M KCl, 0.3 M sucrose, 2 mM DTT, 10 mg/ml CHAPS, 0.5 μg/ml leupeptin, 20 mM Tris-HCl, pH 7.4. The purified receptor reveals a major protein band of 360 kD (greater than 90%) with a minor band of 330 kD (18).

Electron Microscopy

Fixation of samples in 2% glutaraldehyde with 1% tannic acid for thin section electron microscopy was performed as described previously (23, 24). Specimens were examined in a JEOL 100S operated at 80 kV. The magnifications were calibrated using cross grating grid with 2160 lines/mm (Balzers, Nashua, NH).

By optical diffraction analysis, the astigmatism was found to be well-corrected, and the first zero of the contrast transfer function proved to be located such that features larger than 1.5 nm are adequately transferred.

Electron Dose. The total electron dose was estimated from optical density measurement considering the emulsion sensitivity and developing conditions. The dose received by the object during the experiment (30 s) is roughly 30,000 el/nm^2.

Negative Staining

The membrane fraction and ryanodine receptor were negatively stained using somewhat different procedures.

The terminal cisternae fraction (25) was fixed 2–18 h at 4°C in 2.0% (vol/vol) glutaraldehyde by adding 0.25 vol of 8% glutaraldehyde, 100 mM sodium cacodylate, pH 7.2, to the sample suspended in 0.3 M sucrose, 5 mM imidazole, pH 7.4. The fixed sample was diluted to ~1 mg/ml with 0.3 M sucrose, 5 mM imidazole, pH 7.4. 2 μl of the sample were applied to a supporting membrane of a thin carbon film over a 400-mesh grid. Excess sample was removed by touching the grid with the corner of a piece of filter paper. One drop of 1% sodium phosphotungstate, pH 7.2, was applied to the grid. The phosphotungstate solution was freshly filtered through a 0.22-μm pore size Millipore filter attached to a syringe. After a 1-min treatment with the stain, the grid was washed with five drops of staining solution and allowed to remain for 2 min longer. The excess stain was removed by touching with filter paper and the grid was dried under vacuum in the electron microscope to minimize contact with the air.

The Ryanodine Receptor. 2 μl of the sample (~0.3 mg protein/ml) in 10 mg/ml CHAPS, 0.5 M KCl, 0.3 M sucrose, 0.5 μg/ml leupeptin, 2 mM DTT, and 20 mM Tris-HCl, pH 7.4, were applied to a supporting membrane of a very thin carbon film over 400-mesh grid. Excess sample was removed by touching the grid with filter paper. One drop of aqueous 1% uranyl acetate (pH 4.2) was applied to the grid. After 1 min, the grid was washed with 5 drops of 1% uranyl acetate. Excess solution was removed by touching with filter paper, and the grid was dried under vacuum in the electron microscope.

Double Staining

Double staining of the sample was first with 1% uranyl acetate as for negative staining (see above). The grid was washed with several drops distilled water and then treated with 1% lead citrate, pH 11.6, for 3 min (26) and washed again with distilled water. The grid was dried in vacuo in the electron microscope.

Rotary Shadowing

Negative staining is carried out on a smooth carbon surface (32) as described above and then the sample is rotary shadowed at 15°C with 2 nm platinum in a Balzers Freeze-fracture BAF 300 Apparatus (Balzers High Vacuum Corp., Santa Ana, CA).

Image Processing

Micrographs showing the negatively stained receptor in a single-carbon layer preparation were digitized using a Perkin Elmer 1010A microdensitometer with a pixel size of 25 μm, corresponding to 0.58 nm on the object scale. From these digitized fields, 240 images were selected and subjected to correlation alignment with a typical particle as reference (10, 11). The orientation search, done with the direct method (11, 29), showed four peaks of roughly equal size within the 360° range, indicating overall fourfold symmetry. We systematically used the first peak for particle alignment to avoid enhancing asymmetric components. This procedure, which was repeated using the averaged image from the first alignment as reference, is equivalent to fourfold symmetrization. After this second step of alignment, a final average and a variance map (11) were computed.

Results

The purified ryanodine receptor from skeletal muscle can be observed using several different methods of sample preparation for electron microscopy. Using the negative staining technique, both positive and negative images can be observed in the same field (17, 18). Negative stained structures (Fig. 1 *a*) approximate squares (25.6 nm/side ± 1.92; $n = 72$) (17, 18). With uranyl acetate (Fig. 1), the structures by positive image appear as squares (21.4 nm/side ± 2.3; $n = 208$) (18) (Fig. 1, *b* and *c*). Most relevant, additional ultrastructure detail is revealed by negative staining (Fig. 1 *a* and Fig. 2). The receptor varies in appearance, likely reflecting different orientations of the structure with respect to the plane of the carbon film of the grid. There is an outer region and an inner core, each displaying fourfold symmetry. The inner core is generally denser and appears to have a hole at its center (Fig. 1 *a*). Double staining, first with uranyl acetate and then with lead citrate, leads to a positive image with higher contrast (Fig. 1, *c* and *d*). Substructure of the receptor is reflected by the ordered linear arrays observed in the square face (see *arrowhead* in Fig. 1 c, and enlarged in Fig. 6 *g*).

Detailed substructure of the receptor is best observed in negatively stained images (Fig. 2). The appearance varies from that of a cross to more square-like structure (Fig. 2 *a*). The inner core consists of four subunits (Fig. 2 *b*, encircled structure, and *f*). The outer corners of the square on occasion are observed to have double spikes (Fig. 2, *c* and *g*).

Image processing of the micrographs of the negatively stained receptor (240 images) gave a highly improved image. The averaged receptor (Fig. 2 *h*) shows a central mass divided into four domains with a hole in the center of ~2.0 nm. The sharp division of these domains indicates that the fourfold symmetry imposed in the averaging step holds for the central mass as well. The periphery of the particle has a pinwheel appearance created mainly by the asymmetric lo-

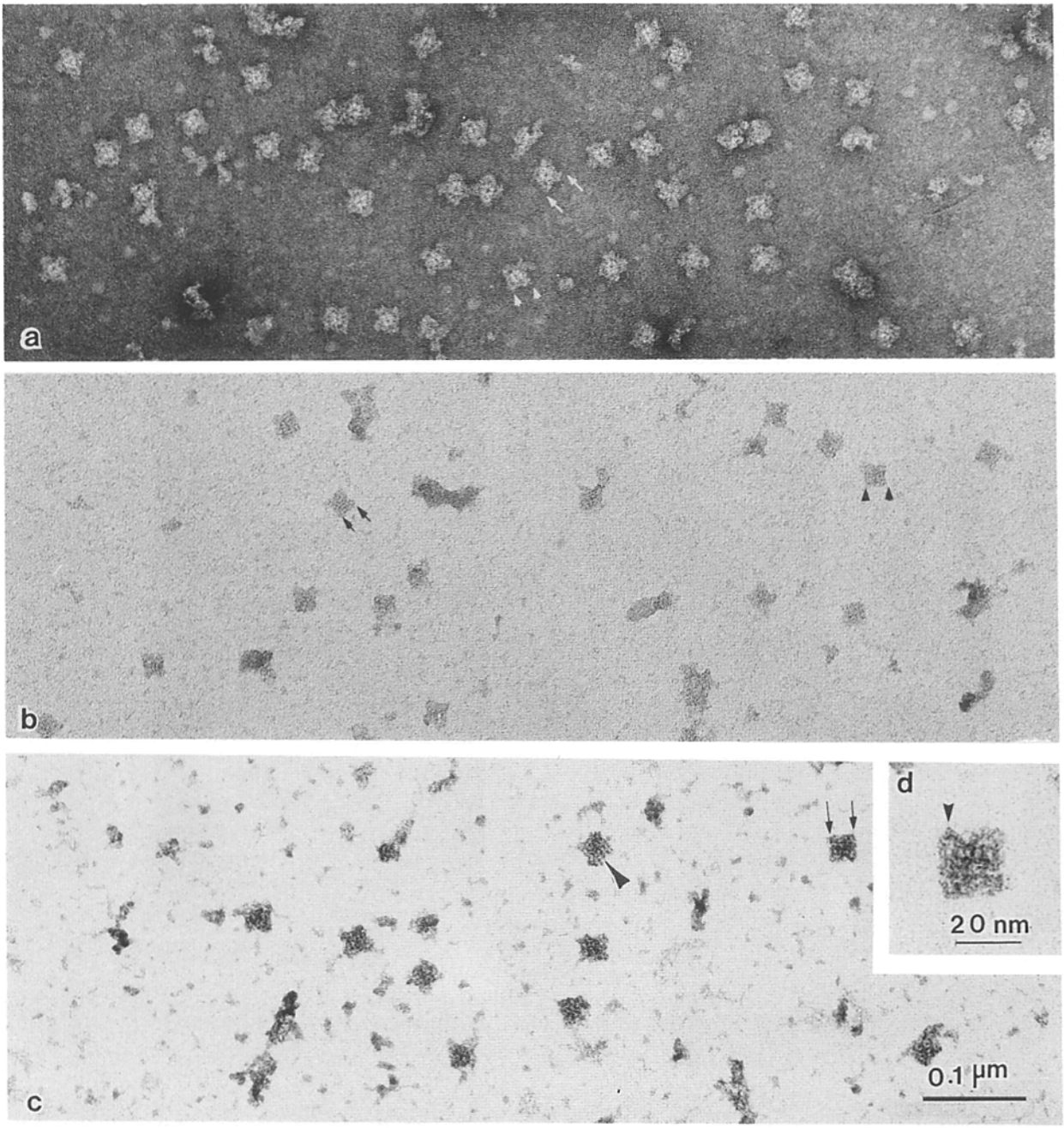

Figure 1. Morphology of the purified calcium release channel/ryanodine receptor. (*a* and *b*) Uranyl acetate staining; (*c* and *d*) Double staining with uranyl acetate and then lead citrate (see Materials and Methods). (*a*) The negative image shows substructure of the receptor which approximates a square of ~22 nm distance between arrowheads and 28 nm between arrows; (*b*) The positive image obtained from the same grid in a nearby field as in Fig. 1 *a*. The sides are 20 nm (between arrows) and 22 nm between arrowheads; (*c*) double staining (see Materials and Methods). Distinct substructure can be observed in the square face (*arrowhead*). (*d*) The square structure is ~25 nm/face with a triangular shape form, discerned in one corner (*arrowhead*).

cation of two stain-excluding masses. The variance map (not shown) suggests that the structure of the central mass strongly varies among the images analyzed. A more detailed picture will emerge from application of multivariate statistical analysis (11, 33) to a larger set of images, which is planned.

Negative staining and rotary shadowing of the channel give complementary images (Fig. 3). By negative staining, most of the field consists of square-like structures and on occasion a rectangular side view can be observed (*arrows*). The rectangle is 25 × 12 nm. A diamond appearance can also be seen by negative staining (see Fig. 3 *b*), suggestive of a side view with the less dense base of the diamond containing the transmembrane portion. Rotary shadowing also reveals square-like structures (Fig. 3 *c*) and less frequently rectangular structures with heavy platinum deposits (16 × 30 nm), suggestive of the side view, (*arrowheads* in Fig. 3 *c*). The heavier shadowing of the rectangular structures (*arrowheads*) indicate a taller structure. This would suggest that the foot

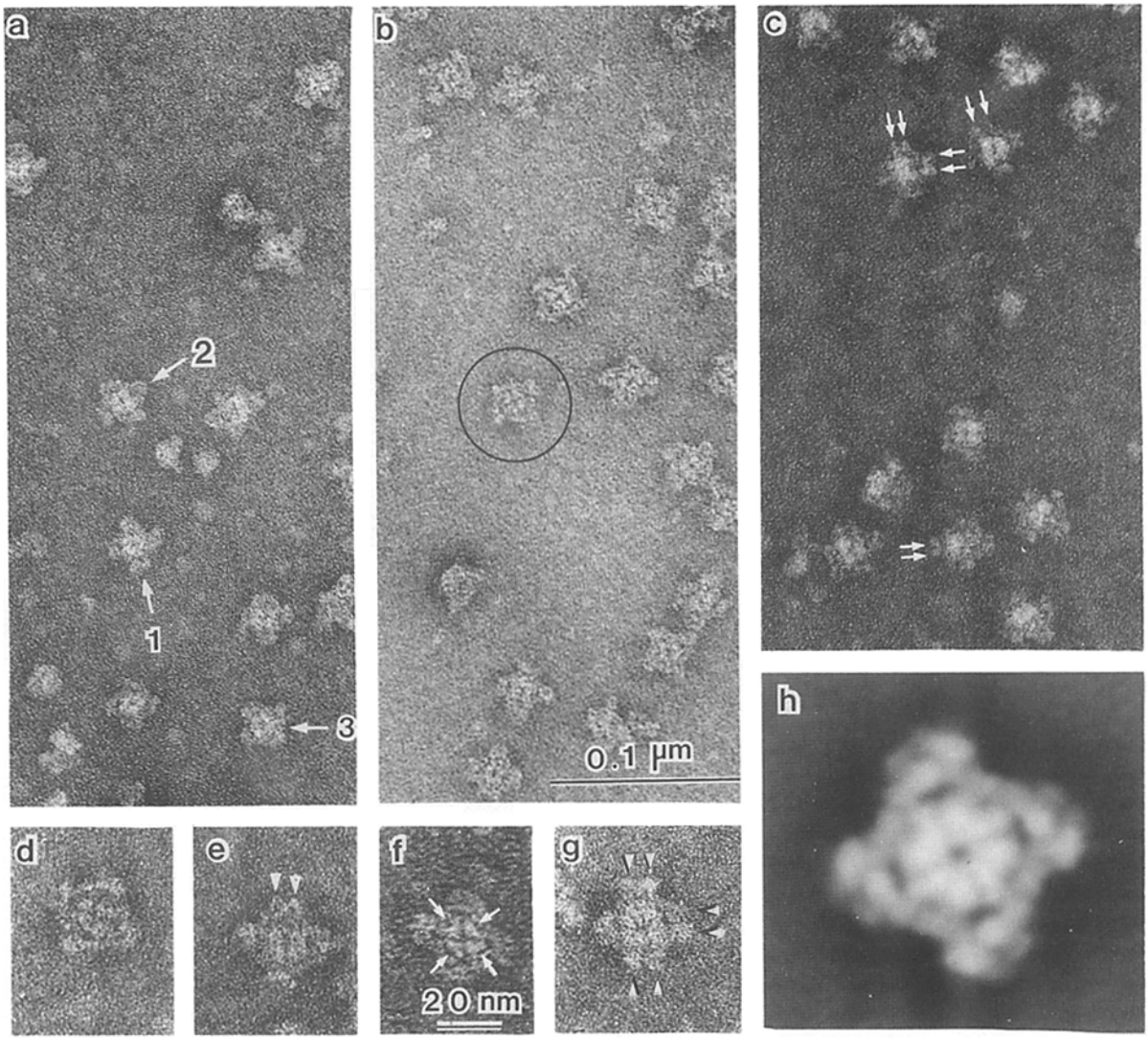

Figure 2. Structure of the ryanodine receptor as viewed by negative staining. In *a–c*, different aspects can be observed. Fourfold symmetry can be seen in both the central dense core and outer region, approximating that of a square. The appearance varies from that of a cross (*1*) to the more square-like appearance (*3*), with intermediate image *2*. In *b* the encircled structure contains a central core consisting of four similar portions, each approximating a triangle and together delineating a cross (see *f*). (*c*) Some of the structures have corners with double triangular appearance (*double arrows*). *d–g* Are negative staining showing different aspects of the receptor. (*d*) Square-like structure exhibiting detail in the center core. (*e*) A double triangle is observed in one corner (*arrowheads*); (*f*) the central portion of the receptor consists of four distinct triangular subunit structures (*arrows*), delineating a cross. In *g*, each of the corners appears to consist of two knob-like projections (*arrowheads*); (*h*) computer averaged top view of the Ca^{2+} release channel/ryanodine receptor obtained by averaging 240 negatively stained images.

structure is usually resting on its square face and less frequently on its rectangular face. On occasion, the structure exhibits a side view (Fig. 3 *d*) suggestive of the diamond structure observed by negative staining (Fig. 3 *b*).

The channel can also be observed by thin section electron microscopy. Both squares (denoted by black arrowheads, Figs. 4, *a* and *b*) and a rectangle (outlined by white arrowheads and by arrows) can be seen (Fig. 4 *b*).

The association of the feet structures with respect to one another has been studied in terminal cisternae in sections tangential to the junctional face membrane (25) (Fig. 5). The feet structures can be observed to associate so as to overlap by ~12 nm rather than to be connected at the pointed corner of the squares. Thus, the channel approximates a square of ~23 nm as compared with 14 nm for the alternating empty square areas. Association of receptors can also be observed by negative staining of the purified receptor. The receptors can be observed to associate in two different modes, i.e., at the extremities of the legs of the cross-like structures (Fig. 5 *d*) and at the corners of the squares (Fig. 5 *e*). The former leads to a smaller intervening square space than the latter.

Ultrastructural detail of the association of feet structures with the junctional face membrane of terminal cisternae can be observed in thin sections (Fig. 6). The side view of the receptor approximates a rectangle in sections normal to the membrane. Typically, the receptor looks wedge-shaped, be-

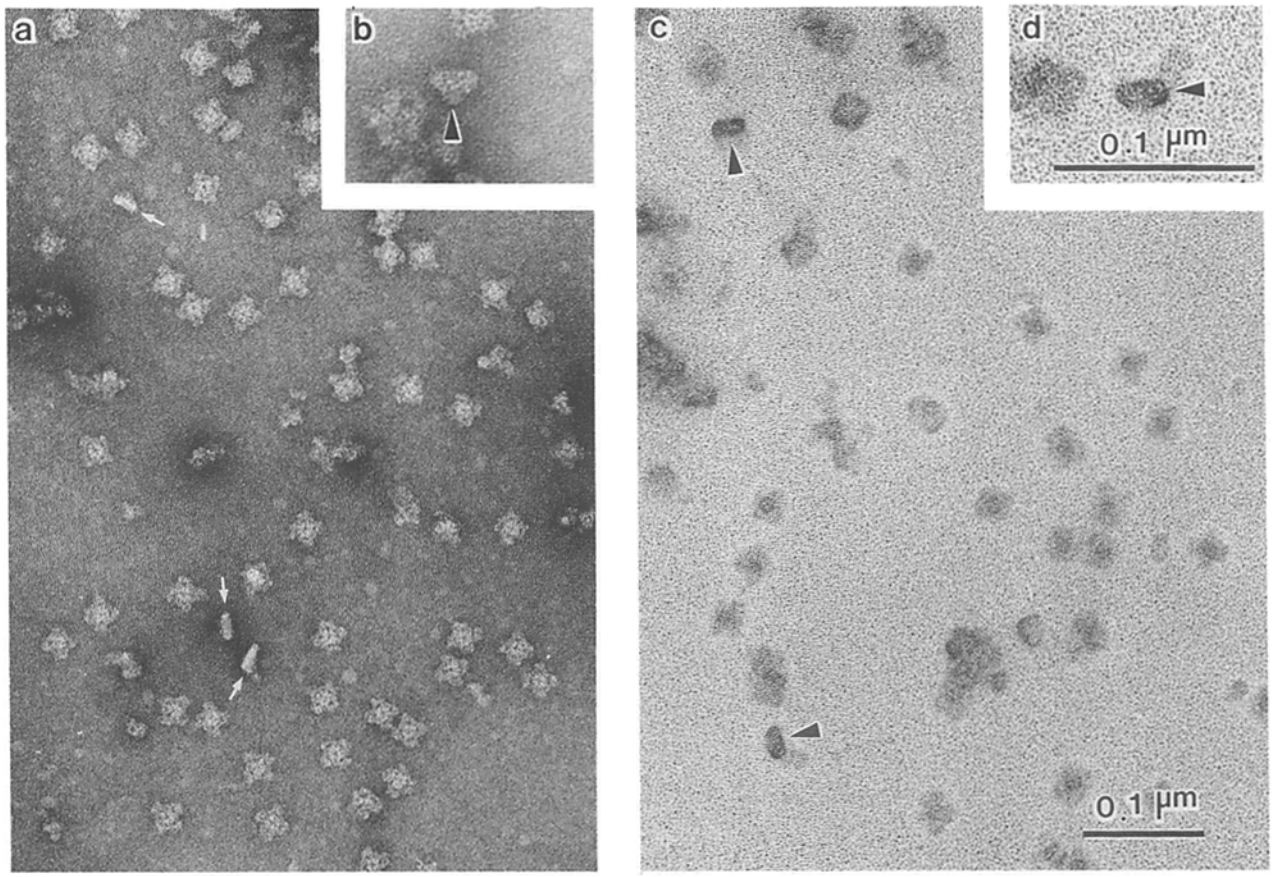

Figure 3. Comparison of the ryanodine receptor by negative staining and by rotary shadowing. (*a* and *b*) Negative staining. (*a*) Most of the field contains different aspects of the square-like structures (~25 nm/side). A rectangular structure is also seen, suggestive of a side view, 25 nm × 12 nm (denoted by arrows). (*b*) The inset (*arrowhead*) contains a diamond structure with the less dense base portion (*arrowhead*) suggestive of the transmembrane portion. (*c* and *d*) Rotary shadowing. (*c*) Most of the images approximate squares. In addition, heavy shadow can be observed in rectangles 16 × 30 nm (*arrowheads*). The inset (*d*) at higher power has a rectangular/diamond appearance (*arrowhead*) (compare with *b*).

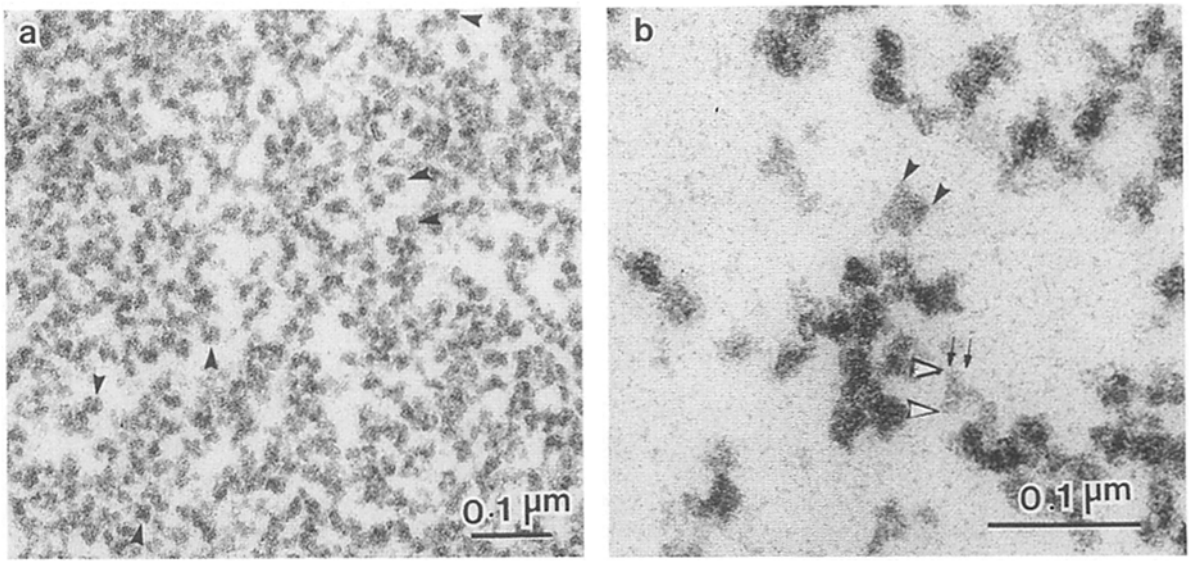

Figure 4. Thin section electron microscopy of the purified receptor. (*a*) At lower power, square structures can be observed (*arrowheads*); (*b*) at higher power, squares can be observed, with dimensions of ~27 nm between arrowheads; a rectangular structure is denoted by two white arrowheads (26 nm) and two arrows (13 nm).

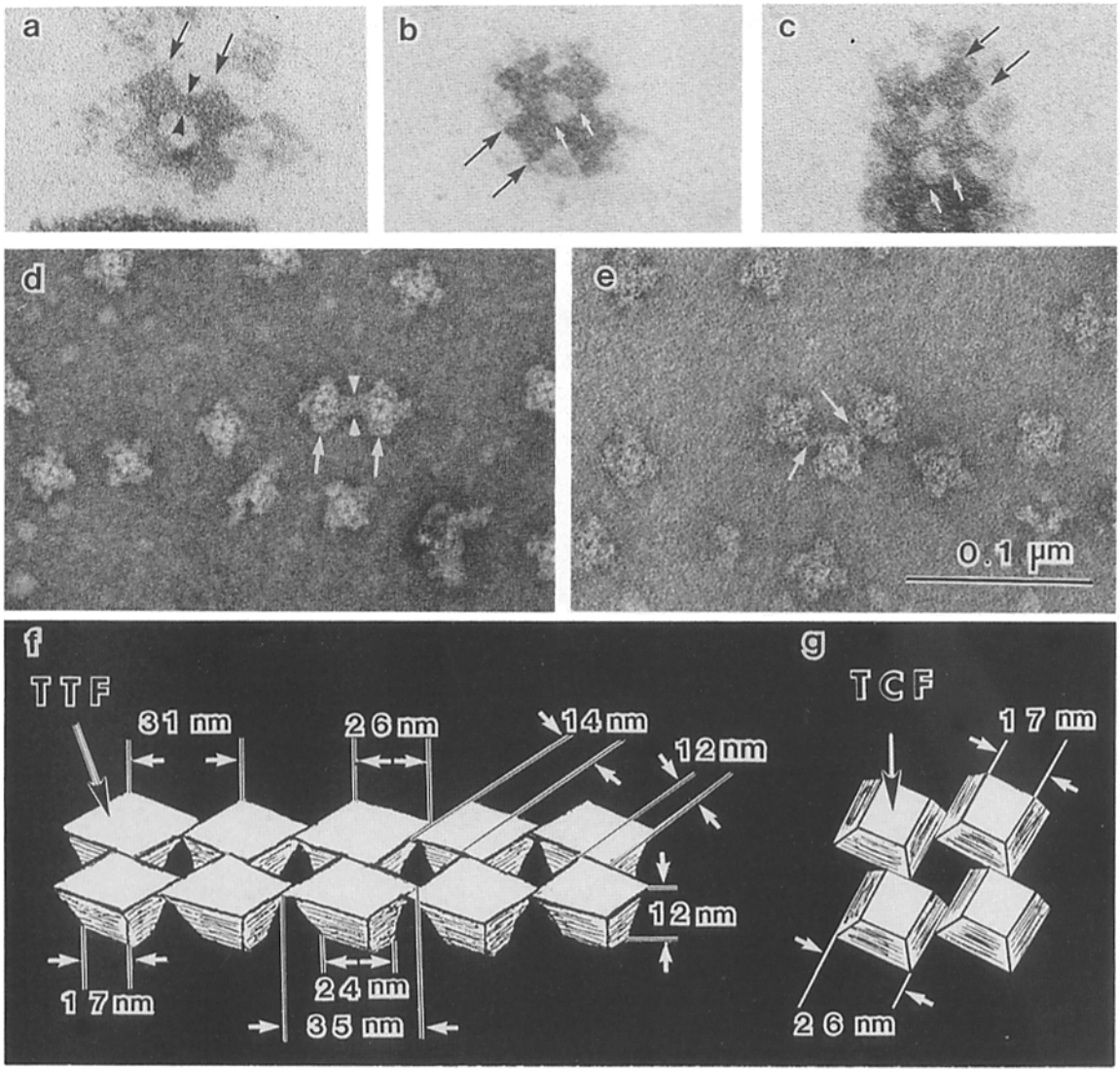

Figure 5. Arrangement of feet structures. (*a–c*) Thin sections tangential to the surface of the junctional face membrane of terminal cisternae vesicles showing arrangement of feet structures. The connection between feet structures deviates from a checkerboard array, that is, the connection is not at a pointed corner but there is ~12-nm overlap (Fig. 6 *a*, space between the arrowheads). The repeat distance between arrows is 31 nm. The foot structure is 23 nm on a side (Fig. 6, *b* and *c*) (distance between dark arrows) whereas the inner clear area approximates a square of 14 nm (*white arrows* in Fig. 6, *b* and *c*). In the purified receptor, by negative staining (*d* and *e*), feet structures can be observed to connect; in *d* two cross-like structures connect via the legs of the cross, 12 nm (between *white arrowheads*), and in (*e*) the square-like structures associate approximately at the corners, giving an overlap of 8 nm (*white arrows*). A diagrammatic representation of the arrangement of feet structures in the junctional face membrane is shown in *f* and *g*. Two features can be noted: (*A*) in the transverse tubule face (*TTF*) (upper face) in *f*, equivalent to the portion which associates with transverse tubule, shows substantial overlap of the sides of the feet structures (26 nm/side) to enclose alternating spaces (14-nm squares) in *f*; and (*B*) the sides of the receptors are tapered so that the terminal cisternae face (*TCF*), the face equivalent to the junctional face membrane (upper face in *g*) approximates a smaller square (~17 nm), with concomitant larger intervening space (*g*).

ing wider at the distal face than at the plane of insertion into the junctional face membrane (arrowheads in Fig. 6, *a* and *b*, and diagrammatically shown in *i*). Occasionally, the width appears broadest midway (Fig. 6, *c* and *d*), suggesting symmetry with respect to the midplane parallel to the square faces of the foot structure (see Fig. 6 *j*). This view is less frequent and may be referable to a section diagonal to the corners of the square of the foot structure reflecting protrusions at the corners (see Fig. 6 *g*).

Detailed fine structure in the form of linear arrays can sometimes be seen in the foot structure in cross-section (Fig. 6 *f*). The periodicity can be related to such detail in the square face of the foot structure observed by double staining (Fig. 1 *d* and 6 *g*). The linear arrays usually run parallel normal to the plane of the membrane and sometimes oblique to the membrane and with respect to one another. Six such linear arrays make up the width of the square face, ~24 nm or 4 nm/repeat (Fig. 6 *g*). The linear arrays and periodicity

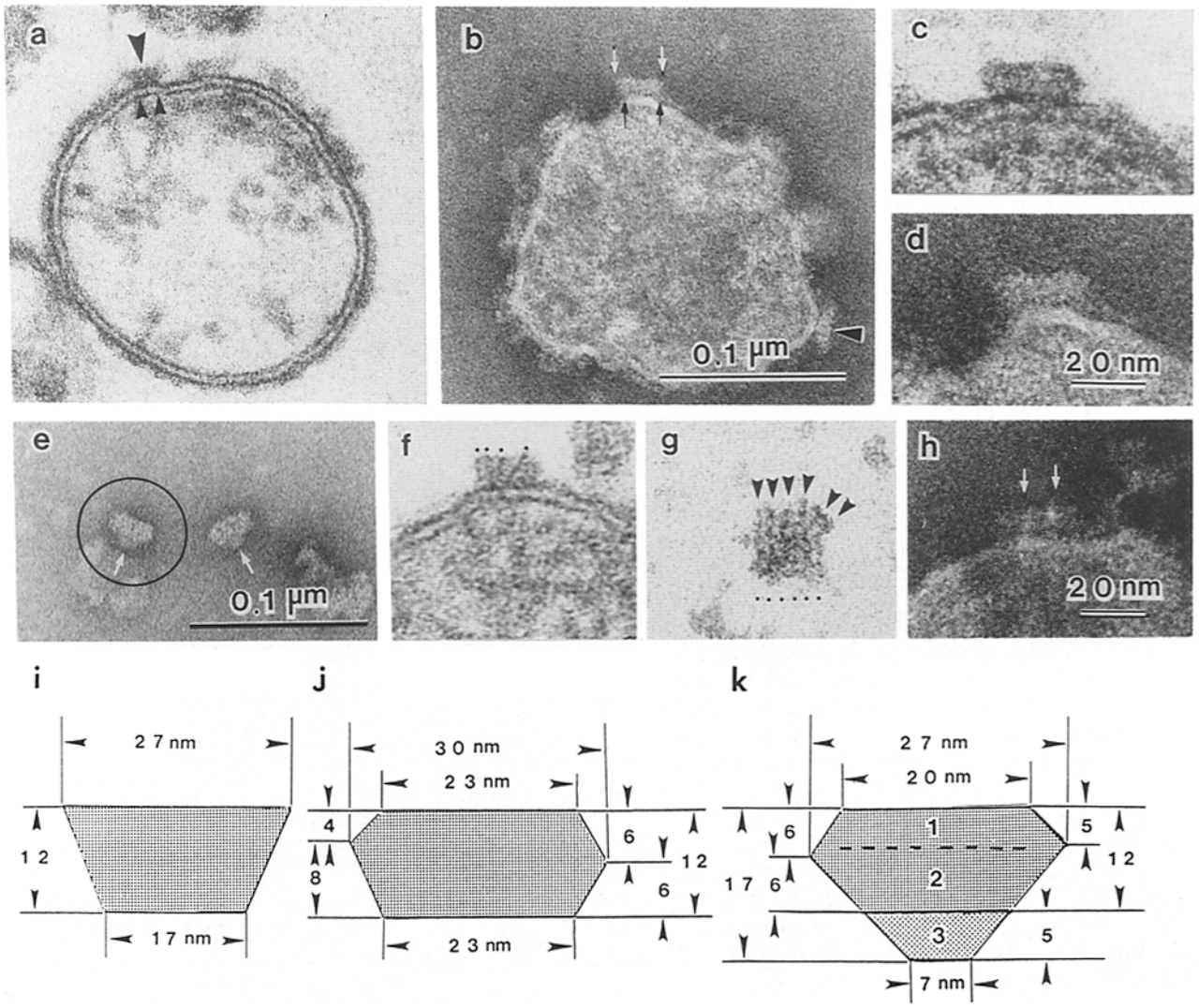

Figure 6. Electron micrographs of terminal cisternae with emphasis on the junctional face membrane. In the thin section in *a*, the side view of the feet structures can be observed in the junctional face membrane. The feet structures have the appearance of a trapezoid. The foot structure (*large arrowhead*) is ~27 nm on the distal (transverse tubule) face and 17 nm proximal, to the membrane surface (terminal cisternae face) (between arrowheads). The foot structure extends 12 nm from the surface. In *b*, negative staining, a similar trapezoid can be observed in the side view of the feet structures by negative staining (*arrowhead*). The arrows point to a foot structure of somewhat different dimensions. The trapezoid is 27 nm (*white arrow*) × 19 nm (*black arrows*). (*c* and *d*) Foot structures with a diamond-like appearance in thin section and by negative staining, respectively. (*e–h*) are higher magnification with emphasis on the association of the feet structures with the membrane. (*e*) Diamond-like structure observed by negative staining. The arrows point to the less dense base portion of diamond which is suggestive of the transmembrane spanning region. (*f*) Thin section shows substructure detail of the receptor in the form of linear arrays of particles; frequently the linear arrays are parallel to one another and normal to the membrane and othertimes they are skew. Of special note, the particles extend to the central electron lucent layer of the junctional face membrane. This matching of periodicity is suggestive of transmembrane extension. (*g*) Similar periodicity (4 nm) of the linear arrays, six/face, can be observed in the square face of the isolated foot structure by double staining (compare with *f*). (*h*) Negative staining of the foot structure. Note denser vertical regions with 12 nm periodicity. (*i–k*) Diagrammatic representation of side views of foot structure. (*i*) Trapezoidal appearance (see *arrowheads* in *a* and *b*); (*j*) side view broader at midline (see *c* and *d*); (*k*) diamond-like appearance characteristics of isolated receptor (see *e* and 3, *b* and *d*); the receptor is depicted as consisting of three segments: *1* and *2* are referable to the junctional region containing the transverse tubule (*1*) and terminal cisternae (*2*) faces, respectively; (*3*) is the transmembrane portion (in the junctional face membrane of terminal cisternae).

match that in the central lucent layer of the membrane (Fig. 6 *f*), suggesting that the foot structure extends through the junctional face membrane.

Discussion

The morphological description of the triad junction and the characterization of the feet structures in junctional association in situ are largely referable to Franzini-Armstrong and her co-workers (12, 13). Other aspects suggestive of bridging processes have also been described (see e.g., 4, 9, 28). The isolation of the terminal cisternae fraction made possible more direct visualization of the feet structures in the junctional face membrane, in vitro (25). More recently, the foot

structure has been characterized in greater detail using freeze-drying and rotary shadowing. A four subunit structure was described and adjacent feet structures were observed to be offset by half a subunit rather than directly connected corner to corner (5).

Our study provides the first detailed ultrastructure of the isolated ryanodine receptor which is now known to be equivalent to the calcium release channel of SR. Extensive detail can be observed by negative staining far beyond the simple appearance of a square-like structure which had been previously reported (17, 18, 25). Further, an enhanced image of the channel was obtained by image processing of the negatively stained structure which contains significant detail of the receptor surface image. More direct information is also provided with respect to the juxtaposition of feet structures to one another and new information with respect to the orientation of the channel in the membrane.

Several methods of sample preparation give complementary appearances. Three different views of the receptor can be observed. (*a*) Square-like structures (~26 nm/side) reflect the face tangential to the junctional face membrane. (*b*) The rectangular face (26 × 12 nm) is referable to the side view. This correlates with the width of the foot structure extending from the membrane, which has been measured from thin section electron microscopy of terminal cisternae to be 12 nm. (*c*) The cross-sectional appearance of the receptor in the shape of a diamond is new. It is observed in the isolated receptor by both negative staining (Fig. 3 *b*), as well as rotary shadowing (Fig. 3 *d*). The less dense base portion of the diamond appearance of the isolated receptor (Figs. 3, *b* and *d*, and 6 *e*) is suggestive of the transmembrane region.

As far as we are aware, the double staining technique to examine ultrastructure of macromolecular assemblies as used in this study is new. It appears to have a great deal of potential for obtaining ultrastructure detail in positive image. The double staining of the isolated receptor displays a new ultrastructure of the channel, i.e., six parallel arrays of particles/square face (Fig. 6 *g*). The periodicity can also be observed in thin section in the side view of the foot structure (Fig. 6 *f*) in the terminal cisternae. Most significant, our studies provide convincing morphological evidence of receptor substructure.

The juxtaposition of the feet structures with respect to one another in the junctional face membrane has also been observed with greater clarity. The structure is not quite a checkerboard array since the lucent spaces between the receptors are smaller squares of 14 nm/face than the receptor (~23 nm/face). This is a consequence of overlap of the receptor by 12 nm rather than being connected at the pointed corners of the square (see Fig. 5). However, the feet structures usually appear tapered with the wider square face being the one that associates with the transverse tubule membrane, and the smaller squares associated with the terminal cisternae. This would suggest that the intervening spaces on the terminal cisternae side are larger and continuous with the space surrounding the sarcomere at the junctional face so that calcium ions can readily diffuse out from the junctional gap (Fig. 5, *f* and *g*).

Thus far, two ion channels, the acetylcholine receptor (30) and the gap junction (31) have been characterized morphologically by electron microscopy and image reconstruction. The detailed three-dimensional structure of the calcium release channel from SR will require image reconstruction analysis. Our studies suggest that this should be feasible.

We are pleased to acknowledge the valuable input from Dr. Terrence Wegenknecht of The New York State Department of Health, and helpful discussions with Dr. Chris Chadwick, Dr. Gerald Stubbs, and Dr. Loren Hoffman (Vanderbilt University).

This work was supported in part by grants from the National Institutes of Health (NIH) DK 14632 and by the Muscular Dystrophy Association to S. Fleischer, and NIH 1 R01 GM 29169 to J. Frank. Dr. Makoto Inui is Investigator of the American Heart Association Tennessee Affiliate.

Received for publication 12 January 1988, and in revised form 21 March 1988.

References

1. Caswell, A. H., and J. P. Braunschweig. 1984. Identification and extraction of proteins that compose the triad junction of skeletal muscle. *J. Cell Biol.* 99:929–939.
2. Chu, A., A. Saito, and S. Fleischer. 1987. Preparation and characterization of longitudinal tubules of sarcoplasmic reticulum from fast skeletal muscle. *Arch. Biochem. Biophys.* 258:13–23.
3. Chu, A., P. Volpe, B. Costello, and S. Fleischer. 1986. Functional characterization of junctional terminal cisternae from mammalian fast skeletal muscle sarcoplasmic reticulum. *Biochemistry.* 25:8315–8324.
4. Eisenberg, B. R., and R. S. Eisenberg. 1982. The T-SR junction in contracting single skeletal muscle fibers. *J. Gen. Physiol.* 79:1–19.
5. Ferguson, D. G., H. W. Schwartz, and C. Franzini-Armstrong. 1984. Subunit structure of junctional feet in triads of skeletal muscle. A freeze-drying, rotary shadowing study. *J. Cell Biol.* 99:1735–1742.
6. Fleischer, S. 1985. Sarcoplasmic reticulum and other membranes in the regulation of muscle contraction and relaxation, a multilevel approach. *In* Structure and function of sarcoplasmic reticulum. S. Fleischer and Y. Tonomura, editors. Academic Press, Inc. New York. 119–145.
7. Fleischer, S., and Y. Tonomura, editors. 1985. Structure and Function of Sarcoplasmic Reticulum. Academic Press, Inc. New York.
8. Fleischer, S., E. M. Ogunbunmi, M. C. Dixon, and E. A. M. Fleer. 1985. Localization of Ca^{2+} release channels with ryanodine in terminal cisternae of sarcoplasmic reticulum of fast skeletal muscle. *Proc. Natl. Acad. Sci. USA.* 82:7256–7259.
9. Forbes, M. S., and N. Sperelakis. 1982. Bridging junctional processes in couplings of skeletal, cardiac, and smooth muscle. *Muscle and Nerve.* 5:674–681.
10. Frank, J., W. Goldfarb, D. Eisenberg, and T. S. Baker. 1978. Reconstruction of glutamine synthetase using computer averaging. *Ultramicroscopy.* 3:283–290.
11. Frank, J., A. Verschoor, and M. Boublik. 1981. Computer averaging of electron micrographs of 40S ribosomal subunits. *Science (Wash. DC).* 214:1353–1355.
12. Franzini-Armstrong, C. 1980. Structure of sarcoplasmic reticulum. *Fed. Proc.* 39:2403–2409.
13. Franzini-Armstrong, C., and G. Nunzi. 1983. Junctional feet and membrane particles in the triad of a fast twitch muscle fiber. *J. Muscle Res. and Cell Motil.* 4:233–252.
14. Hymel, L., M. Inui, S. Fleischer, and H. G. Schindler. 1987. Purified skeletal muscle ryanodine receptor forms Ca^{2+}-activated multisubunit Ca^{2+} channels in planar bilayers. *Proc. Natl. Acad. Sci. USA.* 85:441–445.
15. Imagawa, T., J. S. Smith, R. Coronado, and K. P. Campbell. 1987. Purified ryanodine receptor from skeletal muscle sarcoplasmic reticulum is the Ca^{2+}-permeable pore of the calcium release channel. *J. Biol. Chem.* 262:16636–16643.
16. Inui, M., and S. Fleischer. 1988. Purification of ryanodine receptor from sarcoplasmic reticulum. *Meth. Enzymol.* 157:490–505.
17. Inui, M., A. Saito, and S. Fleischer. 1987. Purification of the ryanodine receptor and identity with feet structures of junctional terminal cisternae of sarcoplasmic reticulum from fast skeletal muscle. *J. Biol. Chem.* 262:1740–1747.
18. Inui, M., A. Saito, and S. Fleischer. 1987. Isolation of the ryanodine receptor from cardiac sarcoplasmic reticulum and identity with the feet structures. *J. Biol. Chem.* 262:15637–15642.
19. Meissner, G. 1986. Ryanodine activation and inhibition of the Ca^{2+} release channel of sarcoplasmic reticulum. *J. Biol. Chem.* 261:6300–6306.
20. Mitchell, R., P. Palade, and S. Fleischer. 1983. Purification of morphologically intact triad structures from skeletal muscle. *J. Cell Biol.* 96:1008–1016.
21. Miyamoto, H., and E. Racker. 1982. Mechanism of calcium release from skeletal muscle sarcoplasmic reticulum. *J. Membr. Biol.* 66:193–201.
22. Peachey, L. D., R. H. Adrian, and S. R. Geiger, editors. 1983. Section 10: Skeletal Muscle. *In* Handbook of Physiology. American Physiological Society, Bethesda.

23. Saito, A., C.-T. Wang, and S. Fleischer. 1978. Membrane asymmetry and enhanced ultrastructural detail of sarcoplasmic reticulum revealed with use of tannic acid. *J. Cell Biol.* 79:601–616.
24. Saito, A., S. Seiler, and S. Fleischer. 1984. Alternations in the morphology of rabbit skeletal muscle plasma membrane during membrane isolation. *J. Ultrastruct. Res.* 86:277–293.
25. Saito, A., S. Seiler, A. Chu, and S. Fleischer. 1984. Preparation and morphology of SR terminal cisternae from rabbit skeletal muscle. *J. Cell. Biol.* 99:875–885.
26. Sato, T. 1968. A modified method for lead staining of thin sections. *J. Electron Microsc.* 12:158–159.
27. Smith, J. C., R. Coronado, and G. Meissner. 1985. Sarcoplasmic reticulum contains adenine-nucleotide-activated calcium channels. *Nature (Lond.).* 316:446–449.
28. Somlyo, A. V. 1979. Bridging structures spanning the junctional gap at the triad of skeletal muscle. *J. Cell Biol.* 80:743–750.
29. Steinkilberg, M., and H. J. Schramm. 1980. Eine verbesserte drehkorrelationsmethode für die Strukturbestimmung biologischer Makromolecüle durch Mittelung elektronenmikroskopischer Bilder. *Hoppe-Seyler's Z. Physiol. Chem.* 361:1363–1369.
30. Stroud, R. M. 1987. Topological mapping and the ionic channel in an acetylcholine receptor. *Soc. Gen. Physiol. Ser.* 41:67–75.
31. Unwin, P. N. T., and G. Zampighi. 1980. Structure of the junction between communicating cells. *Nature (Lond.).* 283:545–549.
32. Valentine, R. C., B. M. Shapiro, and E. R. Stadtman. 1968. *Biochemistry.* 7:2143–2152.
33. Van Heel, M., and J. Frank. 1981. Use of multivariate statistics in analysing the images of biological macromolecules. *Ultramicroscopy.* 6:187–194.